Research Article Journal of Orthoptera Research 2026, 35(1): 191–196

Microsatellite markers for the praying mantid *Tenodera sinensis* (Mantodea, Mantidae) and the demonstration of multiple paternity

Scott B. Ferguson[1], Colm P. Roster[1], Michael O'Hara[1], Alaina J. Hogue[1], Hannah J. Reid[1], William D. Brown[1]

1 Department of Biology, The State University of New York at Fredonia, Fredonia, USA.

Corresponding author: William D. Brown (brownw@fredonia.edu)

Academic editor: Editor | Received 25 July 2025 | Accepted 22 November 2025 | Published 2 March 2026

https://zoobank.org/CB50202F-67F9-435F-9A78-16CB0F5CBF7A

Citation: Ferguson SB, Roster CP, O'Hara M, Hogue AJ, Reid HJ, Brown WD (2026) Microsatellite markers for the praying mantid *Tenodera sinensis* (Mantodea, Mantidae) and the demonstration of multiple paternity. Journal of Orthoptera Research 35(1): 191–196. https://doi.org/10.3897/jor.35.166724

Abstract

The praying mantid *Tenodera sinensis* (Saussure, 1871) is widely distributed and a popular species for studying many aspects of mantid biology. In this study, ten microsatellite loci were characterized both by hybridization capture from genomic DNA and by bioinformatic identification of tetranucleotide repeats from a draft genome. The number of alleles per locus ranged from 4 to 13, and heterozygosity ranged from 0.35 to 0.94. Allelic variation from a single locus was used to demonstrate multiple paternity in a wild clutch of *T. sinensis*.

Keywords

Chinese mantid, genetic markers, molecular ecology, paternity, population genetics, simple sequence repeats

Introduction

Tenodera sinensis (Saussure, 1871) (Mantodea: Mantidae) is a praying mantid native to Asia that was introduced to North America in the late 1800s (Laurent 1898) and is possibly now the most widely distributed temperate zone mantid (Hurd 1999, Jensen et al. 2009). This large-bodied mantid has become an important species for studying mantid ecology (Hurd 1999), behavior (e.g., Liske and Davis 1984), and physiology (e.g., Bertsch et al. 2019). Many recent studies on the breeding biology of *T. sinensis* have focused on the evolutionary ecology of sexual cannibalism (e.g., Lelito and Brown 2006, Brown and Barry 2016, O'Hara and Brown 2021). Details of the breeding system, particularly patterns of sperm usage and opportunities for multiple mating, are expected to have important consequences for the fitness costs of sexual cannibalism (Buskirk et al. 1984, Barry and Kokko 2010). We report here on the development of microsatellite DNA markers for assessing paternity, measuring sperm precedence, and investigating the genetic structure of wild populations of *T. sinensis*.

Microsatellite markers have been previously developed for three mantid species (Attard et al. 2009, Watanabe et al. 2011, Nagata et al. 2022), but primers developed from these studies either failed to amplify or failed to yield polymorphic loci in our samples of *T. sinensis*. Thus, we developed novel microsatellite markers for *T. sinensis*. Our work began prior to the publication of a draft genome of *T. sinensis* (Goldberg et al. 2024). Thus, we initially used biotinylated microsatellite probes and streptavidin-coated beads to isolate microsatellites from the genomic DNA of *T. sinensis* collected from a wild population in western New York, USA. We screened 80 candidate clones by polymerase chain reaction (PCR) and sequenced 40 clones containing large inserts. This sequencing yielded 16 novel microsatellites for which we designed PCR primers. Six of these loci successfully amplified and were polymorphic.

Although the microsatellites identified by hybridization capture yielded valuable information on paternity and population structure, many were dinucleotide repeats that suffered significant stutter upon amplification. Therefore, subsequent to the publication of the draft genome of *T. sinensis* by Goldberg et al. (2024), we bioinformatically identified several tetranucleotide repeat loci that amplify with high fidelity and low stutter.

Allelic variation at microsatellite loci was analyzed using capillary electrophoresis and genes amplified from 11 to 23 individual mantids. We quantified the number of alleles, estimated expected (H_e) and observed (H_o) heterozygosity per locus, and we tested for linkage disequilibrium and deviations from Hardy-Weinberg equilibrium. We then used a single microsatellite locus for a preliminary analysis of multiple paternity on offspring that emerged from a single wild *T. sinensis* ootheca.

Materials and methods

Microsatellite identification by hybridization capture from genomic DNA.—We used the Zymo Tissue/Insect Miniprep kit (Zymo Research, Seattle, WA) for DNA extraction from 50 mg of adult mantis tissue. DNA concentrations were read using a BioSpec-nano spectrophotometer (Shimadzu, Kyoto, Japan) measuring absorbance

Copyright *Scott B. Ferguson et al.* This is an open access article distributed under the terms of the Creative Commons Attribution License (CC BY 4.0), which permits unrestricted use, distribution, and reproduction in any medium, provided the original author and source are credited.

at 260 nm. We fragmented genomic DNA samples (500 ng) using the NEBNext Ultra II FS fragmentation system (New England Biolabs, Ipswich, MA). The enzyme mixture randomly fragments the genome, repairs the ends, and adenylates the 3′ termini. The reaction was carried out according to the manufacturer's recommendations for 3–10 minutes. The fragmented genome was then purified using AMPure XP magnetic beads (Beckman Coulter, Brea, CA) and eluted in 10 µl of water.

Two complementary oligonucleotides were hybridized to form linkers. A 22-mer sequence (5′– CTCTTGCTTACGCGTGGACTAT–3′, 100 µM) was hybridized to a 24 *Mlu*I linker with a 5′ phosphate and a 3′ amino blocking group to promote directional ligation to the adenylated genomic fragments (5′–TAGTCCACGCGTAAGCAAGAGCAC–3′, 100 µM). The oligos were hybridized in a 10 µl reaction at 10 µM of each oligo in 1x NEB T4 DNA Ligase buffer (New England Biolabs, Ipswich, MA) by heating to 95 °C and cooling at 1 °C per minute until they reached 25 °C. We ligated the T/A overhangs of the linkers and the fragmented gDNA in a reaction consisting of 8.5 µl of gDNA, 3 µl of annealed linkers, and 11.5 µl of 2X Blunt/TA Ligase master mix (New England Biolabs, Ipswich, MA). The ligation reaction was cleaned up using AMPure XP magnetic beads and eluted in 40 µl of TE buffer.

Following Attard et al. (2009), biotinylated microsatellite probes (CA_{10} and GA_{10} at 1 µM each) were hybridized to the gDNA-linker fragments in 12x SSC buffer with 0.2% SDS. DNA strands were denatured at 95 °C and cooled at a rate of 5 °C per minute until 25 °C was reached. Hydrophilic Streptavidin magnetic beads (New England Biolabs, Ipswich, MA) (75 µl) were washed twice with 250 µl TE buffer and twice with 150 µl 6x SSC buffer with 0.1% SDS. The hybridized probe/gDNA complexes (120 µl) were added to the Streptavidin beads resuspended in 150 µl of 6x SSC buffer with 0.1% SDS and incubated for 30 minutes at room temperature. Subsequent washes of 2x SSC with 0.1% SDS, 1x SSC with 0.1% SDS at room temperature, and 1x SSC with 0.1% SDS at 47 °C were performed in triplicate. The beads were resuspended and boiled in 200 µl of TE buffer for 5 minutes. The resulting solution was concentrated using a Zymo Clean and Concentrate column and eluted in 25 µl of water (Zymo Research, Seattle, WA). Microsatellites were amplified by PCR using 500 nM of the 21-mer primer described above, 10 µl of the eluted DNA, and Illustra PureTaq Ready-to-Go PCR beads (Cytiva, Wilmington, DE). Standard Taq polymerase protocol was used, and amplification was checked with a 0.8% agarose gel stained with ethidium bromide.

PCR amplicons were cloned into the TOPO-TA cloning kit (ThermoFisher Scientific, Waltham, MA). Blue-white screening and colony PCR using the 21-mer primer sequences identified colonies with large inserts. Colonies containing large inserts were sequenced by Genewiz Inc. (South Plainfield, NJ) using the T3 primer.

ApE software (Davis and Jorgensen 2022) was used to analyze the sequencing electropherograms. Linker and vector sequences were removed and microsatellites were identified using the Simple Sequence Repeat Identification Tool (http://www.gramene.org/). Primers were designed to be approximately 20 nucleotides long, have 50% GC content, and contain two GC clamps on the 3′ ends. An M13 primer binding site (5′–TGTAAAACGACGGCCAGT–3′) was added to the 5′ end of the forward primer, and a PIG tail (5′-GTTTCTT-3′) was added to the 5′ end of the reverse primer to promote complete adenylation (Brownstein et al. 1996, Schuelke 2000).

Microsatellite identification from draft genome of Tenodera sinensis.—A draft genome of the Chinese mantid was published in 2024 (Goldberg et al. 2024). Due to the challenges we encountered with stuttering of the dinucleotide microsatellites that were isolated by hybridization capture (see Results and Discussion), we searched this draft genome for tetranucleotide repeat microsatellites using the Krait tool (Du et al. 2018). The FNA file was downloaded from NCBI and imported into Krait v1.5.1, and microsatellites with motifs larger than 3 and repeats greater than 9 but less than 25 were identified. M13-tailed forward and PIG-tailed reverse primers were designed to nine loci. Four amplified well and were deemed to be polymorphic based on a sample of nine nymphs from four unique ootheca.

Microsatellite screening through PCR and capillary electrophoresis.—We isolated genomic DNA from whole nymphs or distal tarsal segments from a middle leg for microsatellite characterization using 50 µl of QuickExtract DNA extraction solution (Biosearch Technology, Hoddesdon, UK). PCR experiments were performed with 2X OneTaq DNA Polymerase (New England Biolabs, Ipswich, MA) with standard master mix buffer. PCR conditions included M13 primer binding site forward primer at 50 nm, PIG tail reverse primer and 6-FAM conjugated M13 primer at 500 nm, and from 5–15 ng of gDNA dependent on the concentration of isolated DNA sample. Loci CRAM8, CRAM 10, CRAM 12, SDDS4, SK1, and SK18 followed the following touchdown PCR program: an initial denaturation at 95 °C for 3:00, then seven cycles of 94 °C for 0:30, 62 °C for 0:30 (with each cycle reducing the annealing temperature by 0.5 °C), and 72 °C for 0:40. The program then performed 26 cycles of 94 °C for 0:30, 58 °C for 0:30, and 72 °C for 0:40 followed by a final incubation at 72 °C for 5:00. The GPMS, QHMS, and SHMS loci followed the following touchdown PCR program: an initial denaturation at 94 °C for 3:00, then 15 cycles of 94 °C for 0:30, 65 °C for 0:30 (with each cycle reducing the annealing temperature by 0.7 °C), and 72 °C for 0:40. The program then performed 15 cycles of 94 °C for 0:30, 54 °C for 0:30, and 72 °C for 0:40 followed by a final incubation at 72 °C for 5:00. The ETMS locus amplified well with a non-touchdown PCR cycle of 94 °C for 3:00, then 30 cycles of 94 °C for 0:30, 54 °C for 0:30, and 72 °C for 0:30 followed by a final incubation at 72 °C for 5:00.

PCR products (1 µl) were mixed with 8.5 µl of formamide and 0.5 µl LIZ1200 DNA ladder (Applied Biosystems, Waltham, MA), and the DNA was denatured at 95 °C for 5 minutes followed by transfer to ice. Capillary electrophoresis was carried out on an Applied Biosystems Genetic Analyzer 3500 running a 50 cm capillary array and POP-7 polymer. The samples were injected at 1600 V for 8 seconds and run at 19,500 V for 1,600 seconds. Microsatellite analysis was performed using GeneMapper software V 5.0 (Thermo Fisher Scientific, Waltham, MA).

We used Genepop (version 4.7.5; Raymond and Rousset 1995, Rousset 2008) to estimate expected (H_e) and observed (H_o) heterozygosities per locus and to test for linkage disequilibrium and deviations from Hardy-Weinberg equilibrium.

Results and discussion

We identified six variable microsatellite loci from the genomic DNA of *T. sinensis*, with the number of alleles ranging from 4 to 10 and heterozygosities varying from 0.48 to 0.94 (Table 1). Fig. 1 shows sequence maps for two of these loci (see Suppl. material 1 for maps of all 10 loci). CRAM8 is a compound repeat with imperfect TG and AG repeat motifs. SK18, in contrast, has a simple TG dinucleotide motif that is uninterrupted in our archetype allele. Two of the six loci, SK18 and SDDS4, showed significant departure from Hardy-Weinberg equilibrium. Both had a deficit in heterozygosity, which may indicate inbreeding or the presence of null alleles (alleles that fail to amplify). No evidence of linkage disequilibrium was detected in paired comparisons between loci (all $P > 0.05$ after Bonferroni correction).

PCR amplification of the dinucleotide microsatellites such as SK1 tended to yield notable stutter (Fig. 2A), which can make genotyping imperfect. Dinucleotide alleles that stuttered were assigned using the following criteria: The largest peak, both in terms of molecular weight and height, was considered the true size of the allele. In Fig. 2A, for example, an allele that stuttered typically produced a very tall peak followed by progressively shorter stutter peaks spaced 2 bases apart. In this example, there are two series of stuttering peaks with a tall peak to the right and a smaller stutter to the left. In cases of heterozygosity of more closely spaced alleles, "constructive interference" was observed where the largest allele produced a somewhat shorter peak height, followed by a taller peak 2–4 bp to the left where the primary peak of the lower molecular weight allele and the stutter peaks from the higher molecular weight allele overlapped to produce a taller spike.

Given the issue of imperfect genotyping due to stutter, we identified four additional variable tetranucleotide microsatellite loci from sequences in the draft genome of *T. sinensis*, with the number of alleles ranging from 9 to 13 and heterozygosity varying from 0.70 to 0.85 (Table 1). Two of these also showed a significant departure from Hardy-Weinber equilibrium due to a deficit in heterozygosity. We found significant linkage disequilibrium for loci SHMS and QHMS ($P = 0.0016$) but for no other loci (all $P > 0.05$). SHMS and QHMS are located approximately 188 Kb apart on the same contig (JAYMZH010000002.1), so this result is not surprising. These tetranucleotide loci amplify with considerably less stutter (Fig. 2B, C) and enable unambiguous allele assignment.

To demonstrate use of a polymorphic microsatellite locus in paternity analysis, we extracted genomic DNA from 16 nymphs hatched from a single ootheca collected from a wild population in Fredonia, NY. We analyzed the parentage of these nymphs by genotyping the CRAM12 locus (Fig. 3). The progeny array

Table 1. Primer sequences and characteristics of 10 *Tenodera sinensis* microsatellite loci.

Locus	Primer sequences (5′-3′)	Repeat motif	N_g	N_a	Size range (bp)	H_o	H_e	GenBank Accession no.
Identified by hybridization with genomic DNA								
CRAM8	(F)ACTTGTGTGTAAGTGCGCCTG (R)GTGAATGAGTGAGTGAGTGG	$(TG)_{12}(AG)_{10}$*	11	6	240–297	0.73	0.67	PV963100
CRAM10	(F)AGGGCAGTTTAGGGTGGAGG (R)AATAGCGCCCGGATGTTTAGG	$(TC)_{15}(AC)_{27}$	16	5	475–484	0.94	0.78	PV963101
CRAM12	(F)TTGCCTGTTTGCGTGTTTGC (R)GCTTTAGATCGATATCGAGAG	$(TCAC)_{19}$	21	5	224–267	0.76	0.69	PV963102
SK1	(F)TTAATTTGGGACTTCGGACC (R)ACTCTGCAACAGCTCATACG	$(TG)_{38}$	19	10	208–247	0.89	0.85	PV963103
SK18	(F)GCAACCACGTATTGGAAATGG (R)TGGCATTGTGCATTACGGAG	$(TG)_{37}$	21	4	171–189	0.48	0.69†	PV963104
SDDS4	(F)GGGGAAGTATTGTATTTCACCC (R)TATGACTACAAGGGCTGTCG	$(TCAC)_{46}$	17	8	284–321	0.35	0.70†	PV963105
Identified from a genomic draft sequence (Goldberg et al. 2024)								
ETMS	(F)GGAACTGGGTCTTTCTGTTGC (R)TGTCGTATGTATCCGCAGGC	$(TGAG)_{25}$	19	11	435–505	0.74	0.91†	JAYMZH010000019
GPMS	(F)GTTGGTGGACGTTTTCATCCC (R)ATGTTATCGGTAACTGCACTCG	$(AAAT)_{17}$	23	13	252–392	0.7	0.85†	JAYMZH010000010
SHMS	(F)TCTTCAGGCTCTTCCTCACG (R)ATTCCCACATGGTGAAACGC	$(TCAC)_{11}$	20	9	511–588	0.85	0.83	JAYMZH010000002
QHMS	(F)GCCCAAGCAGAAATGATGGG (R)ACACCTGCTCACTTCTCTCC	$(CACT)_{28}$	19	9	374–421	0.79	0.77	JAYMZH010000002

N_g, number of individuals genotyped; N_a, number of alleles; H_o, observed heterozygosity; H_e, expected heterozygosity. Forward primers (F) were tagged with a 5′M13 universal sequence (5′-TGTAAAACGACGGCCAGT-3′) and reverse primers (R) were tagged with a PIG universal sequence (5′-GTTTCTT-3′); sequences shown exclude these portions.

*Imperfect TG and AG motifs.

†Locus significantly deviates from Hardy-Weinberg equilibrium after Bonferroni correction ($P < 0.05$).

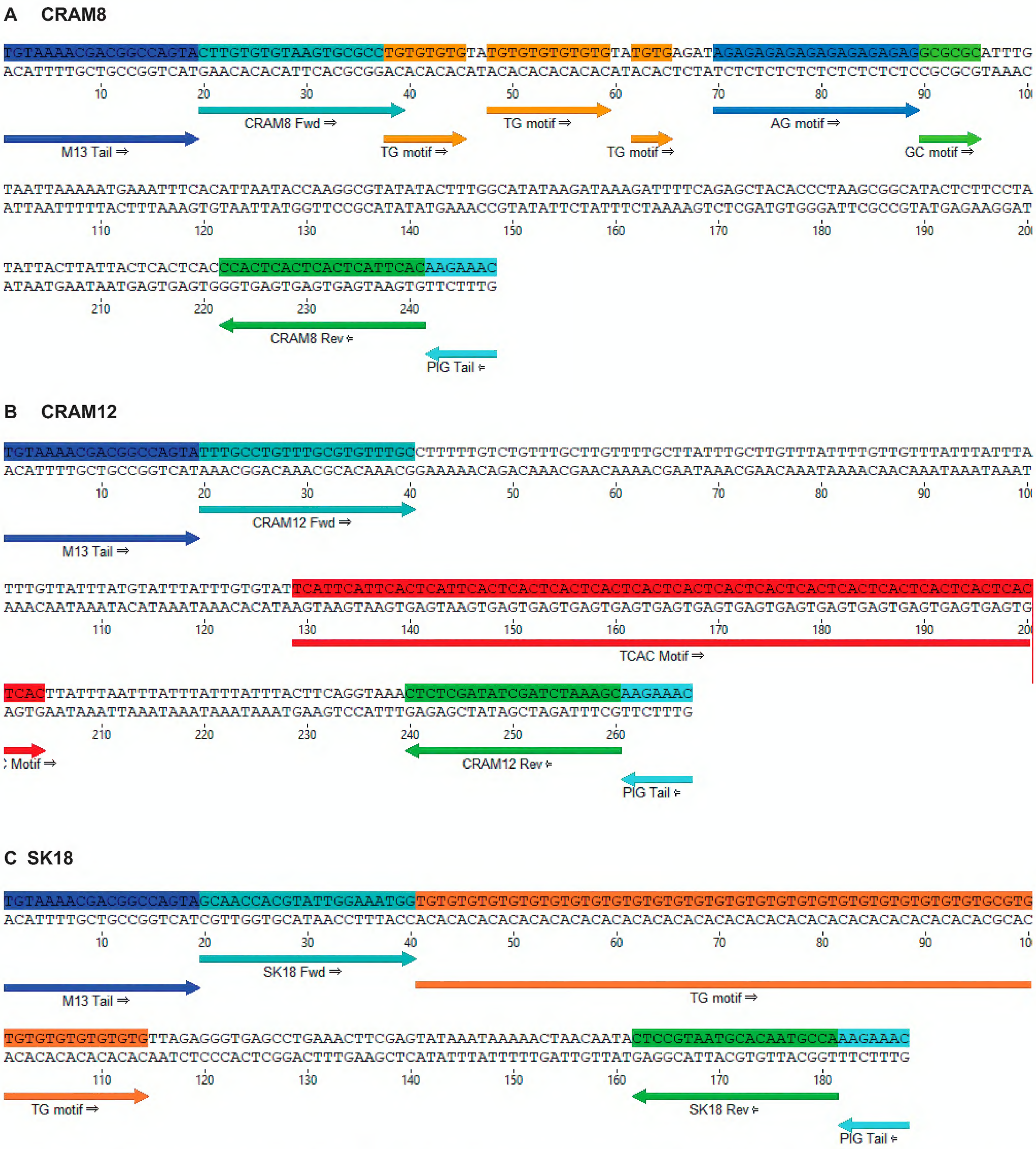
A CRAM8
TGTAAAACGACGGCCAGTACTTGTGTGTAAGTGCGCCTGTGTGTGTATGTGTGTGTGTGTATGTGAGATAGAGAGAGAGAGAGAGAGAGGCGCGCATTTG
ACATTTTGCTGCCGGTCATGAACACACATTCACGCGGACACACACATACACACACACACATACACTCTATCTCTCTCTCTCTCTCTCCGCGCGTAAAC
10 20 30 40 50 60 70 80 90
CRAM8 Fwd ⇒
TG motif ⇒
AG motif ⇒
M13 Tail ⇒
TG motif ⇒
TG motif ⇒
GC motif ⇒
TAATTAAAAATGAAATTTCACATTAATACCAAGGCGTATATACTTTGGCATATAAGATAAAGATTTTCAGAGCTACACCCTAAGCGGCATACTCTTCCTA
ATTAATTTTTACTTTAAAGTGTAATTATGGTTCCGCATATATGAAACCGTATATTCTATTTCTAAAAGTCTCGATGTGGGATTCGCCGTATGAGAAGGAT
110 120 130 140 150 160 170 180 190
TATTACTTATTACTCACTCACCCACTCACTCACTCATTCACAAGAAAC
ATAATGAATAATGAGTGAGTGGGTGAGTGAGTGAGTAAGTGTTCTTTG
210 220 230 240
CRAM8 Rev ⇐
PIG Tail ⇐
B CRAM12
TGTAAAACGACGGCCAGTATTTGCCTGTTTGCGTGTTTGCCTTTTTGTCTGTTTGCTTGTTTTGCTTATTTGCTTGTTTATTTTGTTGTTTATTTATTTA
ACATTTTGCTGCCGGTCATAAACGGACAAACGCACAAACGGAAAAACAGACAAACGAACAAAACGAATAAACGAACAAATAAAACAACAAATAAATAAAT
10 20 30 40 50 60 70 80 90
CRAM12 Fwd ⇒
M13 Tail ⇒
TTTGTTATTTATGTATTTATTTGTGTATTCATTCATTCACTCATTCACTCACTCACTCACTCACTCACTCACTCACTCACTCACTCACTCACTCAC
AAACAATAAATACATAAATAAACACATAAGTAAGTAAGTGAGTAAGTGAGTGAGTGAGTGAGTGAGTGAGTGAGTGAGTGAGTGAGTGAGTGAGTG
110 120 130 140 150 160 170 180 190
TCAC Motif ⇒
TCACTTATTTAATTTATTTATTTATTTACTTCAGGTAAACTCTCGATATCGATCTAAAGCAAGAAAC
AGTGAATAAATTAAATAAATAAATAAATGAAGTCCATTTGAGAGCTATAGCTAGATTTCGTTCTTTG
210 220 230 240 250 260
Motif ⇒
CRAM12 Rev ⇐
PIG Tail ⇐
C SK18
TGTAAAACGACGGCCAGTAGCAACCACGTATTGGAAATGGTGTGTGTGTGTGTGTGTGTGTGTGTGTGTGTGTGTGTGTGTGTGTGTGTGTGTGCGTG
ACATTTTGCTGCCGGTCATCGTTGGTGCATAACCTTTACCACACACACACAC

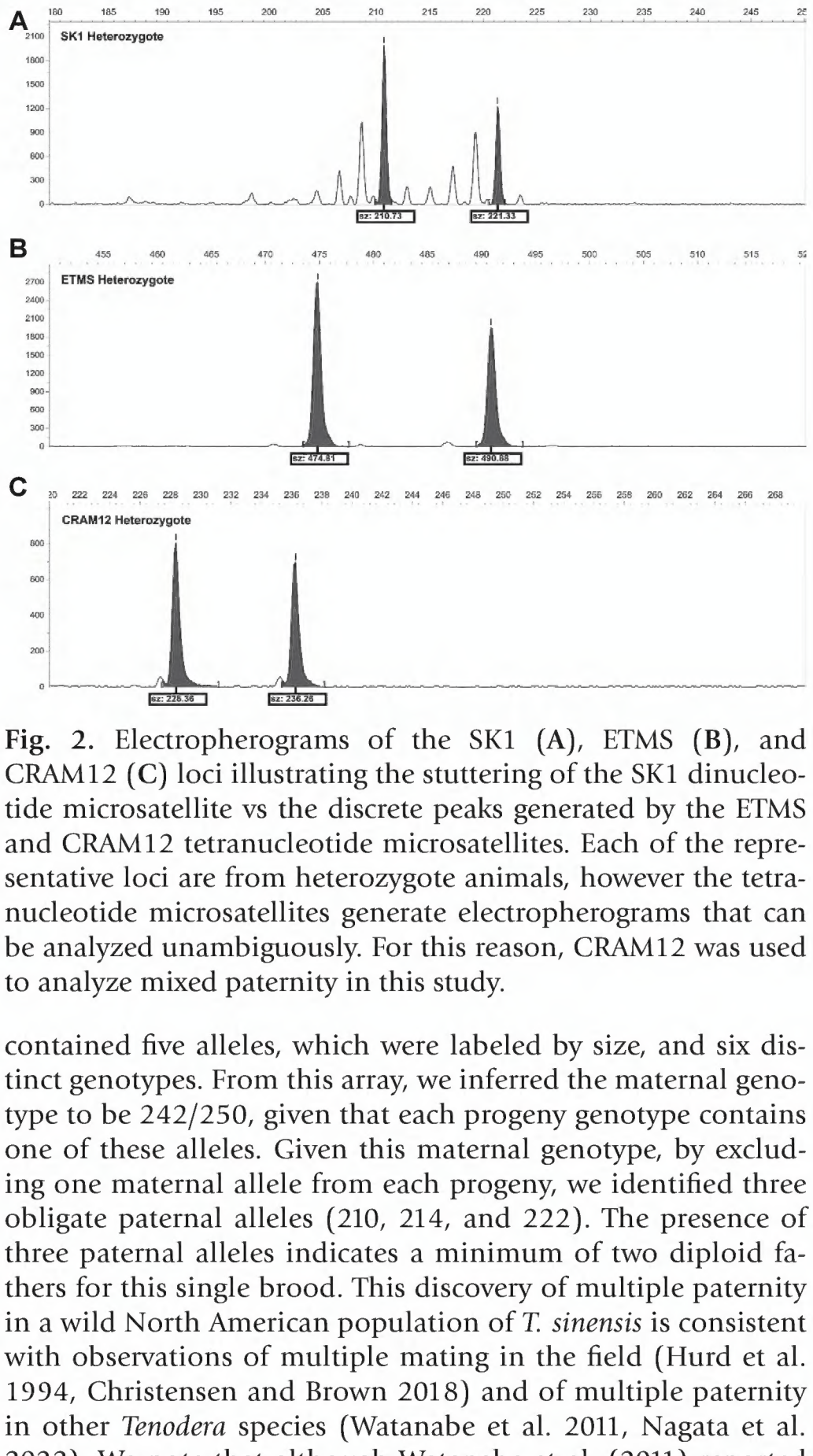

Fig. 2. Electropherograms of the SK1 (**A**), ETMS (**B**), and CRAM12 (**C**) loci illustrating the stuttering of the SK1 dinucleotide microsatellite vs the discrete peaks generated by the ETMS and CRAM12 tetranucleotide microsatellites. Each of the representative loci are from heterozygote animals, however the tetranucleotide microsatellites generate electropherograms that can be analyzed unambiguously. For this reason, CRAM12 was used to analyze mixed paternity in this study.

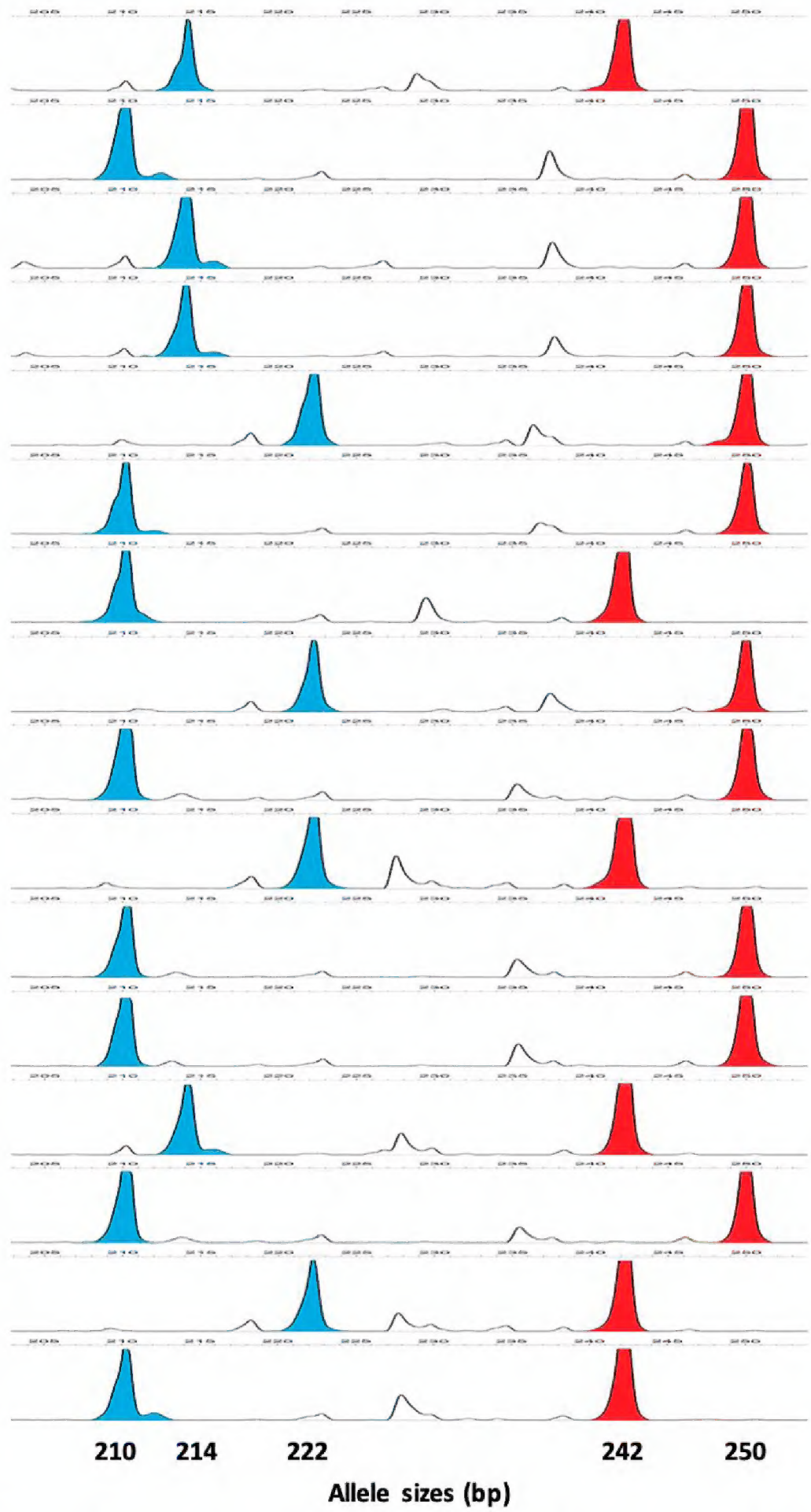

Fig. 3. Using microsatellite locus CRAM12 to screen a single clutch of nymphs for multiple paternity: Each row shows the electropherogram of one nymph from a single ootheca, and thus a common mother, with 16 nymphs in total. Alleles are color coded with putative maternally derived alleles in red and putative paternally derived allele in blue. The presence of three paternally derived alleles indicates a minimum of two fathers in this brood.

contained five alleles, which were labeled by size, and six distinct genotypes. From this array, we inferred the maternal genotype to be 242/250, given that each progeny genotype contains one of these alleles. Given this maternal genotype, by excluding one maternal allele from each progeny, we identified three obligate paternal alleles (210, 214, and 222). The presence of three paternal alleles indicates a minimum of two diploid fathers for this single brood. This discovery of multiple paternity in a wild North American population of *T. sinensis* is consistent with observations of multiple mating in the field (Hurd et al. 1994, Christensen and Brown 2018) and of multiple paternity in other *Tenodera* species (Watanabe et al. 2011, Nagata et al. 2022). We note that although Watanabe et al. (2011) reported multiple paternity in *Tenodera aridifolia* Stoll, 1813, their species may actually have been *T. sinensis*. Phylogenetic work on *Tenodera* (Jensen et al. 2009) showed *T. sinensis* to be a distinct species, sister to *T. aridifolia*, but species in Japan, where Watanabe et al. (2011) collected their samples, were determined to be *T. sinensis*. It is puzzling, however, that the microsatellite marker developed by Watanabe et al. (2011) failed to amplify in our samples of *T. sinensis*.

Conclusion

Herein, we describe the isolation and characterization of ten novel polymorphic microsatellite loci for the praying mantid *T. sinensis*. Among the microsatellites developed from genomic DNA, polymorphism ranged from 4 to 13 alleles, with heterozygosities ranging from 0.35 to 0.94. This amount of variation should make these genetic makers ideal candidates for studying relatedness, breeding biology, and the genetic structure of wild populations of *T. sinensis*. To illustrate this point, we used a single variable locus to demonstrate multiple paternity in a single clutch taken from a wild population of mantids. These loci provide a powerful tool for studying the breeding system, population structure, and evolutionary ecology of wild populations of *T. sinensis*.

Acknowledgements

This work was funded in part by the Department of Biology, SUNY Fredonia, and Fredonia Biology Summer Research Fellowships for AH, CR, and MO. We would also like to acknowledge the work of the Fredonia Molecular Genetics Lab students who contributed to the development of these sequences as part of a course-based undergraduate research experience.

References

Attard CM, Holwell GI, Schwartz TS, Umbers KDL, Stow A, Herberstein ME, Beheregaray LB (2009) Microsatellite markers for the praying mantid *Ciulfina rentzi* (Liturgusidae). Molecular Ecology Resources 9: 1480–1482. https://doi.org/10.1111/j.1755-0998.2009.02718.x

Barry KL, Kokko H (2010) Male mate choice: why sequential choice can make its evolution difficult. Animal Behaviour 80:163–169. https://doi.org/10.1016/j.anbehav.2010.04.020

Bertsch DJ, Martin JP, Svenson GJ, Ritzmann RE (2019) Predatory behavior changes with satiety or increased insulin levels in the praying mantis (*Tenodera sinensis*). Journal of Experimental Biology 222: jeb197673. https://doi.org/10.1242/jeb.197673

Brown WD, Barry KL (2016) Sexual cannibalism increases male material investment in offspring: quantifying terminal reproductive effort in a praying mantis. Proceedings of the Royal Society of London B 283: 20160656. https://doi.org/10.1098/rspb.2016.0656

Brownstein MJ, Carpten JD, Smith JR (1996) Modulation of non-templated nucleotide addition by *Taq* DNA polymerase: primer modifications that facilitate genotyping. BioTechniques 20: 1004–1010. https://doi.org/10.2144/96206st01

Buskirk RE, Frohlich C, Ross KG (1984) The natural selection of sexual cannibalism. American Naturalist 123: 612–625. https://doi.org/10.1086/284227

Christensen T, Brown WD (2018) Population structure, movement patterns, and frequency of multiple matings in the mantid *Tenodera sinensis* (Mantodea: Mantidae). Environ Entomol 47: 676–683. https://doi.org/10.1093/ee/nvy048

Davis MW, Jorgensen EM (2022) ApE, a plasmid editor: a freely available DNA manipulation and visualization program. Frontiers in Bioinformatics 2: 818619. https://doi.org/10.3389/fbinf.2022.818619.

Du L, Zhang C, Liu Q, Zhang X, Yue B (2018) Krait: an ultrafast tool for genome-wide survey of microsatellites and primer design. Bioinformatics 34: 681–683. https://doi.org/10.1093/bioinformatics/btx665

Goldberg JK, Godfrey RK, Barrett M (2024) A long-read draft assembly of the Chinese mantis (Mantodea: Mantidae: *Tenodera sinensis*) genome reveals patterns of ion channel gain and loss across Arthropoda. G3: Genes, Genomes, Genetics 14: jkae062. https://doi.org/10.1093/g3journal/jkae062

Hurd LE (1999) Ecology of praying mantids. In: Prete FR, Wells H, Wells PH, Hurd LE (Eds) The Praying Mantids. Johns Hopkins Press, Baltimore, 43–60.

Hurd LE, Eisenberg RM, Fagan WF, Tilmon KJ, Snyder WE, Vandersall KS, Datz SG, Welch JD (1994) Cannibalism reverses male-biased sex ratio in adult mantids: female strategy against food limitation? Oikos 69: 193–198. https://doi.org/10.2307/3546137

Jensen D, Svenson GJ, Song H, Whiting MF (2009) Phylogeny and evolution of male genitalia within the praying mantis genus *Tenodera* (Mantodea: Mantidae). Invertebrate Systematics 23: 409–421. https://doi.org/10.1071/IS09004

Laurent R (1898) A species of Orthoptera. Entomological News 9: 144–145.

Lelito JP, Brown WD (2006) Complicity or conflict over sexual cannibalism? Male risk-taking in the praying mantis *Tenodera aridifolia sinensis*. American Naturalist 168: 263–269. https://doi.org/10.1086/505757

Liske E, Davis WJ (1984) Sexual behaviour of the Chinese praying mantis. Animal Behaviour 32: 916–917. https://doi.org/10.1016/S0003-3472(84)80170-0

Nagata Y, Nishino H, Kuroda K, Shinohara T, Satomi D, Terada K, Nishimura T, Kuroda T, Inoue Y, Park Y, Takami Y (2022). Reproductive phenology and female mating frequency of the praying mantid *Tenodera angustipennis* in western Japan. Ecological Entomology 47: 423–431. https://doi.org/10.1111/een.13127

O'Hara MK, Brown WD (2021) Sexual cannibalism increases female egg production in the Chinese praying mantid (*Tenodera sinensis*). Journal of Insect Behavior 34: 127–135. https://doi.org/10.1007/s10905-021-09776-y

Raymond M, Rousset F (1995) GENEPOP (version 1.2): population genetics software for exact tests and ecumenicism. Journal of Heredity 86: 248–249. https://doi.org/10.1093/oxfordjournals.jhered.a111573

Rousset F (2008) Genepop'007: a complete reimplementation of the Genepop software for Windows and Linux. Molecular Ecology Resources 8: 103–106.

Saussure H (1871) Mélanges orthoptérologiques. Mémoires de la Société de Physique et d'Histoire Naturelle de Genève 21: 1–214

Schuelke M (2000) An economic method for the fluorescent labeling of PCR fragments. Nature Biotechnology 18: 233–234. https://doi.org/10.1038/72708

Stoll C (1813) Representation exactement colorée d'après nature des spectres ou phasmes, des mantes, des sauterelles, des grillons, des criquets et des blattes: 65.

Watanabe E, Adachi-Hagimori T, Miura K, Maxwell MR, Ando Y, Takematsu Y (2011) Multiple paternity within field-collected egg cases of the praying mantid *Tenodera aridifolia*. Annals of the Entomological Society of America 104: 348–353. https://doi.org/10.1603/AN10035

Supplementary material 1

Author: Scott B. Ferguson, Colm P. Roster, Michael O'Hara, Alaina J. Hogue, Hannah J. Reid, William D. Brown
Data type: pdf
Explanation note: Maps of all ten microsatellite loci for *Tenodera sinensis*.
Copyright notice: This dataset is made available under the Open Database License (http://opendatacommons.org/licenses/odbl/1.0/). The Open Database License (ODbL) is a license agreement intended to allow users to freely share, modify, and use this Dataset while maintaining this same freedom for others, provided that the original source and author(s) are credited.
Link: https://doi.org/10.3897/jor.35.166724.suppl1